

ORIGINAL ARTICLE

A mathematical model of the colon crypt capturing compositional dynamic interactions between cell types

Kieran Smallbone* and Bernard M. Corfe*^{*,†,‡}

*Manchester Centre for Integrative Systems Biology, University of Manchester, Manchester, [†]Molecular Gastroenterology Research Group, Academic Unit of Surgical Oncology, Department of Oncology, University of Sheffield, Sheffield, and [‡]Insigneo Institute, The University of Sheffield, Sheffield, UK

**INTERNATIONAL
JOURNAL OF
EXPERIMENTAL
PATHOLOGY****SUMMARY**

Models of the development and early progression of colorectal cancer are based upon understanding the cycle of stem cell turnover, proliferation, differentiation and death. Existing crypt compartmental models feature a linear pathway of cell types, with little regulatory mechanism. Previous work has shown that there are perturbations in the enteroendocrine cell population of macroscopically normal crypts, a compartment not included in existing models. We show that existing models do not adequately recapitulate the dynamics of cell fate pathways in the crypt. We report the progressive development, iterative testing and fitting of a developed compartmental model with additional cell types, and which includes feedback mechanisms and cross-regulatory mechanisms between cell types. The fitting of the model to existing data sets suggests a need to invoke cross-talk between cell types as a feature of colon crypt cycle models.

doi: 10.1111/iep.12062

Received for publication: 18
December 2012Accepted for publication: 24
September 2013**Correspondence:**

Dr Bernard M. Corfe
Molecular Gastroenterology Research
Group
Academic Unit of Surgical Oncology
Department of Oncology
University of Sheffield
Beech Hill Road
Sheffield, S10 2RX
UK
Tel.: +44-114-271-3004
E-mail: b.m.corfe@sheffield.ac.uk

Keywords

apoptosis, cancer, cell cycle, cell–cell signalling, colon crypt, differentiation, mathematical model

The colon (and small intestine) is lined by many millions of crypts, which serve to increase the surface area of the gut for absorptive and secretory functions, which provide a mechanism for replenishment of cells lost through sloughing and which act in sensing and signalling capacity to monitor luminal contents. The crypt has a slow-dividing, long-lived stem cell compartment at the base, which populates a more actively dividing transit-amplifying compartment, from which cells exit by differentiating into one of the secretory lineages. A further subclass of cells is the enteroendocrine (EEC) compartment, which comprises a small number of cells, but whose role may be significant: for example, most of the postprandial GLP-1 release driving cessation of eating comes from the colon (Anini *et al.* 1999). Likewise, not only other gut hormones (Gunawardene *et al.* 2011) but molecules known to be involved in apoptotic signalling, such as VEGF and VEGF-receptor (Gulubova & Vlaykova 2008)

and Nrp-1 (Yu *et al.* 2011), are expressed in cells of the EEC lineage.

The crypt is therefore a microcosmic model of stem cell differentiation, amplification, differentiation and death. The crypt is thought to be under exquisite regulation in order to maintain a reasonably steady state, but nonetheless retains the ability to shrink or grow in conditions of starvation and to respond to alterations in the large bowel content (Sakata & von Engelhardt 1983; Sakata 1987; Inagaki & Sakata 2005). Changes in crypt composition have been noted in large bowel pathologies; numbers of proliferating cells per crypt are elevated in the macroscopically normal tissues in pericancerous and peri-adenomatous fields (Humphries & Wright 2008); likewise, perturbations in rates of apoptosis may contribute to breakdown of epithelia associated with forms of colitis, or failure to shed in hyperplasia. Our group have previously shown that there are changes in the EEC

compartment in peri-adenomatous fields (Yu *et al.* 2011). The mechanisms underlying this perturbation of crypt dynamics are unclear, but work using xenograft models of colorectal cancer has also shown that there is a change in EEC numbers in the gut mucosa, suggesting a diffusible factor may contribute (Cho *et al.* 2008).

It is logical that small changes in crypt dynamics may, over large amounts of time, lead to the types of macroscopic abnormalities associated with early stages of colorectal disease; however, such changes are not readily identified or captured by empirical methods. Mathematical modelling offers the chance to identify and compute interactions based on observable data and to explore where interactions may be influenced to lead to pathologies. The colonic crypt has previously been subject to a number of modelling efforts, notably the compartmental model from Tomlinson and Bodmer (1995), which has been subject to iterations and adaptations (Johnston *et al.* 2007a). Other models exist and have been reviewed (Johnston *et al.* 2007b; De Matteis *et al.* 2013). The compartmental model has a number of useful features – in particular the compartmental concept relates closely to observable biology and provides a set of semantic terms that are measurable, specifically the model divides the crypt into stem cells (N_0), transit-amplifying cells (N_1) and differentiated cells (N_2) each of which has a rate of apoptosis, and in the case of N_0 and N_1 a rate of exit and replenishment.

However, the model also has limitations, including a term for saturating feedback with no obvious biological meaning. Furthermore, the model does not include an EEC compartment, which we have shown is both biologically important and subject to alteration in proximity to neoplasia. Finally, in common with the majority of models, this is built to approach a numerical steady-state derived from averaged observations. In reality, there will be dynamic relationships between cell types, which exist to maintain the global steady state. Whilst independent observations are made, for example, on changes in numbers or proportions of proliferating cells, of EEC, or of goblet cells (Bernstein *et al.* 2000), few studies have addressed large numbers of endpoints within the same data series. We therefore formally hypothesize that the relationships between cell types in colon crypt compartments will not be constant in strength or direction and that the incorporation of measurements into a crypt model will potentially reveal novel or key regulatory decision points in the crypt cell fate pathway.

Model development

The general workflow for development of the revised model is presented in the supplementary online material, Figure S1. Briefly, we used a pre-existing base model and established goodness of fit to our *in vivo* observed data. We developed a score for fit and then undertook a series of iterative revisions until a model was yielded, which fairly represented the dynamic interactions between cell types in the colon crypt.

The models developed below are made available in Systems Biology Markup Language (SBML, Hucka *et al.* 2003), an exchange format for computer models of biological

processes that is understood by a wide range of software tools. The models are available from the BioModels.net database (Li *et al.* 2010):

Version 0: <http://identifiers.org/biomodels.db/MODEL1306190000>

Version 1: <http://identifiers.org/biomodels.db/MODEL1306190001>

Version 2: <http://identifiers.org/biomodels.db/MODEL1306190002>

Version 3: <http://identifiers.org/biomodels.db/MODEL1306190003>

Parameter values used are presented in Table 1. Simulations and analysis were performed using COPASI (Hoops *et al.* 2006, available from <http://copasi.org/>).

NOTE: until publication the models are available from <http://www.ebi.ac.uk/biomodels/reviews/MODEL1306190000-3/>

Base model

As a base model (version 0), we follow the ‘saturating feedback’ model of Johnston *et al.* (2007a) (other parameterizations of the same model are described in Johnston *et al.* 2007b). The model describes cell population dynamics in the colonic crypt. Let N_0 , N_1 and N_2 denote the numbers of stem, semidifferentiated (transit-amplifying) and fully differentiated cells respectively. Their evolutions are defined by the system

$$dN_0/dt = R_{00} - R_{0X}$$

$$dN_1/dt = R_{01} + R_{11} - R_{1X}$$

$$dN_2/dt = R_{12} - R_{2X}$$

where R_{ii} denotes the rate of symmetric division $N_i \rightarrow 2N_i$, R_{ij} denotes the rate of asymmetric division $N_i \rightarrow N_i + N_j$, and R_{iX} denotes the rate of cell death $N_i \rightarrow \emptyset$.

Reaction rates are defined by Johnston *et al.* as

$$R_{ii} = a_i N_i$$

$$R_{ij} = (b_i + c_i N_i / (N_i + m_i)) N_i$$

$$R_{iX} = d_i N_i$$

Note that most available data from formalin-fixed, paraffin-embedded (FFPE) tissue are based on scores established per hemicypt in section. These measures are one-dimensional (per crypt length) rather than three-dimensional (per crypt volume). Consequently, the base model has been rescaled so that the cellularity $T = \sum N_i$ (the total number of cells per hemicypt) equals 74, rather than 250. It should be noted, however, that there is no explicit spatial dependence defined in the model.

Capacity constraints

The model of Johnston *et al.* suffers from a number of problems. Whilst described as ‘saturating feedback’, it in fact

Table 1 Terms included in successive iterations of the model and their semantic meaning. Parameters used in version 0 derived from Johnston *et al.* (2007a)

| Parameter | v0 | v1 | v2 | v3 | Units | Semantic |
|-----------|------|------|-------|-------|--------------|--|
| a_0 | 0.1 | | | | Per day | |
| a_1 | 0.24 | | | | Per day | |
| b_0 | 0.22 | | | | Per day | |
| b_1 | 0.55 | | | | Per day | |
| c_0 | 1 | | | | Per day | |
| c_1 | 1 | | | | Per day | |
| m_0 | 2.9 | | | | Cell | |
| m_1 | 29 | | | | Cell | |
| d_0 | 0.10 | 0.10 | 0.20 | 0.02 | Per day | Rate of apoptosis from N_0 |
| d_1 | 0.26 | 0.42 | 0.84 | 0.55 | Per day | Rate of apoptosis from N_1 |
| d_2 | 1.8 | 1.1 | 2.2 | 1.9 | Per day | Rate of apoptosis from N_2 |
| d_3 | | | 0.038 | 0.168 | Per day | Rate of apoptosis from N_3 |
| K | | 120 | 120 | 106 | Cell | Crypt capacity |
| r_0 | | 1.8 | 2.0 | 2.0 | Cell per day | Rate of stem cell cycle |
| r_1 | | 5.9 | 6.1 | 10.6 | Cell per day | Rate of proliferating cell cycle |
| p_{01} | | 0.86 | 0.82 | 0.63 | 1 | Rate of exit from stem cell |
| p_{12} | | 0.83 | 0.83 | 0.81 | 1 | Rate of entry into terminal differentiation |
| q_{03} | | | 0.094 | 0.935 | 1 | Maximum probability of N_0 to N_3 division |
| K_{03} | | | 1.60 | 0.78 | Cell | Maximum probability of N_0 to N_3 division |
| K_{0X} | | | 1.60 | 0.15 | Cell | N_3 level at which N_0 apoptosis is half-maximal |
| K_{1X} | | | 1.6 | 15.4 | Cell | N_3 level at which N_1 apoptosis is half-maximal |
| K_{2X} | | | 1.6 | 2.7 | Cell | N_3 level at which N_2 apoptosis is half-maximal |

contains no feedback mechanism: the dynamics of stem cells N_0 are independent of the levels of N_1 and N_2 , for example. Assessment of this model indicated that it could grow or shrink beyond biologically observed sizes through perturbation of a_1 – the cell cycle rate of N_1 (Supplementary online information Figure S2). Furthermore, in a series of stochastic simulations of compartment cellularity, the model frequently lost its stem cell compartment but did not become extinct (Supplementary online data).

The most natural way to incorporate feedback is via capacity constraints. We define the rates of N_0 and N_1 division as $f_i = r_i N_i (1 - T/K)$ where K is the carrying capacity of the crypt, estimated as the largest observed crypt size. This division can then be symmetric ($R_{ii} = p_{ii} f_i$) or asymmetric ($R_{ij} = p_{ij} f_i$) where $p_{00} + p_{01} = 1$ and $p_{11} + p_{12} = 1$. Capacity constraints are typical in biological models. A carrying capacity is used in logistic growth; this is often extended to development of multiple cells or species via the competitive Lotka–Volterra equations.

Parameter values for this model (version 1) are calculated using measured cell counts N_i and assuming transition rates as per the base model. The model improves on the base model by constraining the size of the crypt to within biologically feasible bounds.

Enteroendocrine population

Our previous studies have shown that perturbations in the enteroendocrine cell (EEC) population occur in the macroscopically normal mucosa of subjects with a colorectal lesion, in proximity to the lesion. It has previously been reported that in mice with xenografted colorectal tumours,

there is a similar depression of EEC numbers in the colorectal mucosa (Cho *et al.* 2008). These data suggest that there is potentially an important compositional change in the cell types of the crypt, with EEC being, at the very least, a barometer of such effect. EECs are associated with the expression of receptors, environmental sensors, signalling molecules and receptors such as the apoptosis regulator NRP-1 (Gunawardene *et al.* 2011). Thus, we add a new compartment N_3 to the model (version 2, see Figure 1). We initially estimate – based on observed frequency data (see Table 2) – that 1% of stem cell divisions are used to produce EEC cells.

We define $p_{03} = q_{03} K_{03}/(N_3 + K_{03})$ so that N_3 cells inhibit their own production. Michaelis constants are typically found to be the same order as their substrates (Smallbone & Mendes 2013); thus, as an initial estimate, K_{03} is set to be of the same order as the number of N_3 cells.

The EEC may play a variety of signalling functions in the crypt. For the purposes of this model, we consider that their primary role is the inhibition of apoptosis, and thus, redefine $R_{iX} = d_i A_i N_i$ where the apoptosis rate A_i is given by $A_i = K_{iX}/(N_3 + K_{iX})$. Again, K_{iX} is assumed to be of the same order as N_3 . The model extends the base model by including a small, but biologically important, compartment of EEC, but estimated parameters are improved upon in the next section.

Development of assessment criteria

We have acquired data from the macroscopically normal mucosa of patients with and without neoplasia under an ongoing research project (Corfe *et al.* 2009). In total, 41

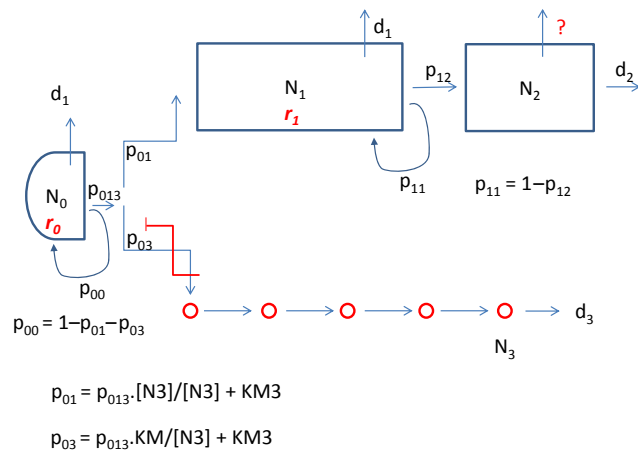


Figure 1 Summary of relationships described in the model, including feedback loops. Parameters are detailed in Table 1 and are an extension of the terms used previously. Briefly, main cell compartments are identified as N_0 (stem cell), N_1 (transit-amplifying cells), N_2 (differentiated cells) and N_3 (enteroendocrine cells). All cell compartments have a rate of apoptotic death (d_0 – d_3 respectively), and N_0 and N_1 have rates of cell cycle (r_0 and r_1 , respectively). N_1 cells may exit into a differentiation pathway with rate p_{12} , or may replenish at rate p_{11} , which sum to unity as the ‘usual’ fates of N_1 cells. N_0 cells may likewise replenish at rate p_{00} or enter a differentiation path at rate p_{013} , which are reciprocal events. Entry into N_1 or N_3 lineages are alternative pathways from p_{013} , and the numbers of N_3 cells feedback to control this fate determination point.

Table 2 Assessment of root mean square fit of model to experimentally derived parameters

| | OBS | v0 | v1 | v2 | v3 |
|---------|-------|------|------|-------|-------|
| N1 | 27 | 44 | 27 | 28 | 30.3 |
| N2 | 46 | 27 | 46 | 46 | 47.9 |
| N3 | 1.6 | | | 1.7 | 1.2 |
| fit | | 0.71 | 0.58 | 0.05 | 0.14 |
| N2 v N1 | –0.24 | 1.00 | 0.08 | 1.00 | –0.31 |
| N3 v N1 | 0.04 | | | 1.00 | 0.04 |
| N3 v N2 | 0.26 | | | 1.00 | 0.00 |
| N1 v T | 0.80 | 1.00 | 0.95 | 1.00 | 0.90 |
| N2 v T | 0.11 | 1.00 | 0.03 | 1.00 | 0.13 |
| N3 v T | 0.06 | | | 1.00 | 0.11 |
| fit | | 5.73 | 0.88 | 13.30 | 0.60 |

Top half of table shows predicted number of cells at steady state for successive modifications to the model, and a comparison to experimentally observed average numbers. The bottom half shows predicted correlations between compartment sizes and experimentally observed correlations. In both cases, a comparison is made using the root mean square fit. Observed data (OBS) were reference values from the normal group in a cross-sectional study (Corfe *et al.* 2009). In all 41 subjects, data were used to determine mean values and Spearman’s correlation coefficients.

subjects were free from pathology. Histology had been undertaken, and numbers of proliferating cells were determined by Ki67 staining (defined as N_1), cellularity (T) by H&E staining and EEC by enterochromaffin staining (N_3).

As the crypt is a dynamic entity with variation in compartment size and cellularity over time, we were able to establish by correlation that some (but not all) compartments had strong positive or negative inter-relationships (Table 2). The strength and direction of these relationships formed a set of assessment criteria for the fit of models to experimental data. We hypothesize that, to capture the dynamic relationship between cell types, it is informative to model their correlation, as well as their average values, as the latter would only lead to a steady-state representation.

A theoretical sample of crypts may be obtained by iteratively allowing independent parameter values to vary by a small proportion δ , calculating the compartmental steady state, then comparing the theoretical correlations obtained with those observed experimentally. In the limit as $\delta \rightarrow 0$, the effect of changing one parameter on a compartment is given by its scaled sensitivity coefficient. Thus, the theoretical correlation is given by the correlation between each compartment’s scaled sensitivity coefficients.

In Table 2, we see that, although steady-state modelling indicated that version 2 of the model was stable, achieved predicted numbers of cells in each compartment and became extinct on loss of stem cells, the strength and direction of relationships was a poor fit to the assessment criteria. Thus, we allow the parameters to vary around their initial estimates, to minimize the distance between the experimental and theoretical correlations, whilst maintaining similar values for compartment size. This was performed in COPASI using its inbuilt Hooke and Jeeves algorithm. We see that the fit (version 3) is much improved.

A summary of the model and its internal relationships is shown in Figure 1.

Example applications

Identifying principal potential mechanism of action of butyrate

To test the value of the model in identification of novel potential mechanisms of action, we sought to identify parameters whose alteration may recapitulate the observed effects of butyrate on crypt composition. Butyrate is a fermentation product of the luminal microbiome, which is implicated as a metabolite of the colon epithelium, as a regulator of cell cycle, of differentiation and of cell death (Hamer *et al.* 2008). Several *in vivo* models have shown that butyrate appears to stimulate proliferation. We surveyed the literature and found that the majority of reports from human studies find a weak and non-significant relationship between the numbers of observed proliferating cells and the faecal butyrate concentration (Bowles & Corfe, in preparation). Our group have recently reported a stronger negative correlation between the enteroendocrine population and faecal butyrate.

We used sensitivity analysis to identify parameters whose variation would confer these relationships at these relative magnitudes (oppositional with greater magnitude per unit

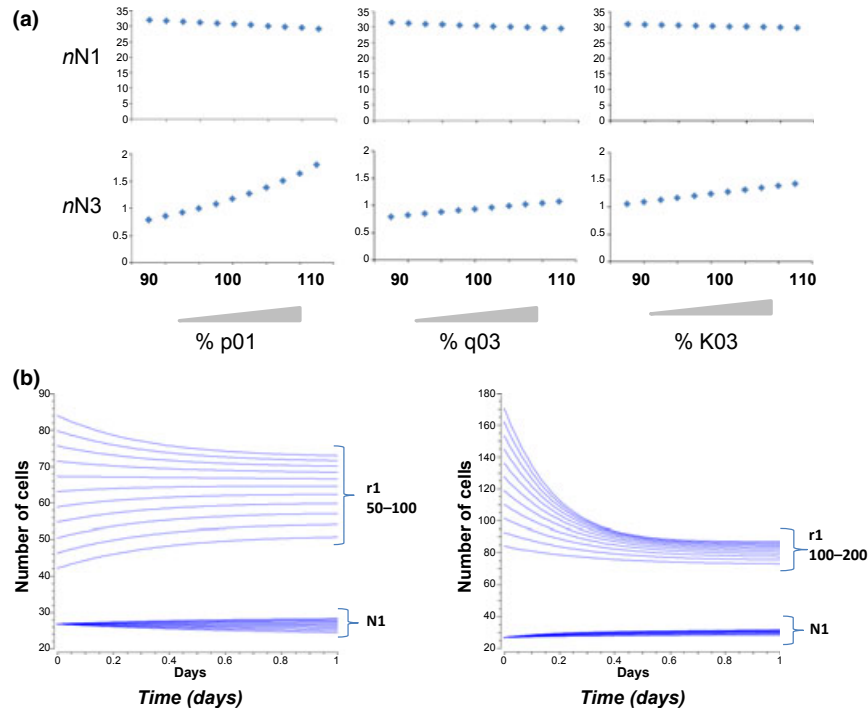


Figure 2 Sample applications of the model. (a) The variations aim to mimic the effects of butyrate upon crypt composition as observed *in vivo*. Predictive outputs consequential to parameter sweeping p_{01} and q_{03} and K_{03} from -10% to $+10\%$ of their value were established for output parameters N_1 and N_3 . (b) The effect of varying cell cycle time (r_1) upon numbers of proliferating cells (N_1) and cellularity (T). Left panel shows progressive 10% decreases in r_1 from 100 to 50%. Right panel shows progressive 10% increases in r_1 from 100 to 200%. Variation of r_1 has little effect on N_1 .

change for N_3 than for N_1). Sensitivity analysis suggested p_{01} , q_{03} and K_{03} all had potential to modify N_1 and N_3 with the opposite directionality and greater magnitude for N_3 (Supplementary Online Information Figure S3). We therefore undertook a parameter scan, within biologically sensible limits (in stepwise increments -15% to $+15\%$). Endpoint data from timecourses are shown in Figure 2a and suggest variation in p_{01} – the rate of exit from the stem cell compartment – may best recapitulate the effects of butyrate. Such predictions cannot exclude the likely pleiotropic effects of butyrate, but fit well with a substantive literature suggesting that butyrate affects the cell cycle.

Effect of varying cell cycle rate on numbers of observed proliferating cells

Changes in the number of proliferating cells in crypts have been observed associated with the presence of a lesion (Sandler *et al.* 2000) and in response to the microenvironment (Holt *et al.* 1996). Such measurements are usually made (in human tissues at least) through classical immunohistochemical approaches. Butyrate has been shown to reduce cell cycle rates *in vitro* in colorectal cancer cell lines and to drive an increase in the number of N_1 cells in normal tissue. It has been induced from this observation that the *in vivo* observation represents an increase in proliferation, which is opposite to the effect on cancer cells *in vitro* and

that this apparently paradoxical effect may be a mechanism of chemopreventive action on transformed cells (Gibson *et al.* 1992; Scheppach *et al.* 1995; Hague *et al.* 1997). We hypothesized that a decrease in cell cycle rate may equally lead to an increase in apparent number of proliferative cells as it may, for example, be the number of cycles, rather than rate, which determines N_1 composition. Such arguments are precedented.

We used our model to undertake a parameter scan of cell cycle rate (r_1) and to measure its effect on numbers of cells in the N_1 compartment (Figure 2b). r_1 was varied between half and double its baseline value. There was no effect of alteration on the N_1 compartment. These data suggest that the cell cycle rate may not be a principle determinant of size of the N_1 compartment in the crypt.

Discussion

The colonic crypt is an attractive target for modelling for a number of reasons – it encapsulates a cycle from stem cell through proliferation, differentiation and death, it is highly regulated, and perturbations in this regulatory process are at the root of early colorectal carcinogenesis, a major cause of cancer mortality.

We have shown that an established model of the colon crypt was unsuited to the analysis and interpretation of our data sets as follows: (i) the absence of a cell subtype

(enteroendocrine cells) which we have previously shown to become deranged in proximity to a colorectal lesion (ii) the model was not size-limited and (iii) the direction of relationships between cell types did not mimic those observed *in vivo*. We sought to use the features of the base model, notably compartmental organization, and then cell fate decisions from each compartment, and to evolve this to our purpose. By exploring the direction and strength of relationships between cell compartment types in an existing data set, as opposed to using global data, we have identified oppositional relationships that needed to be incorporated into the model. It should be noted that the model is built around data generated in one dimension (hemicrypt scores). This is usual for histopathology, and our model is therefore compatible with raw data from human samples; however, this limitation should be noted when comparing against established spatially, rather than histopathologically, motivated 2-d and 3-d models of the crypt (see, for example, Buske *et al.* 2011; Dunn *et al.* 2012; Mirams *et al.* 2012; Pin *et al.* 2012).

We have deliberately sought throughout the developmental steps in modelling to ensure semantic clarity of terms. This allows incorporation into hypermodels or linking of this model to other models (Fishwick 2012), which is to the benefit of the modelling community and ensures that the model has biological meaning and that it is useable and manipulable by biologists.

Two applications of the model have been shown – in the identification of parameters which may account for the observed compositional impact of butyrate upon crypt cell types and for the effects of variation of cell cycle rate. These approaches allow deduction about effects of microenvironmental factors, for example that the assumption that increased proliferation observed in response to butyrate is indicative of an increase in cell cycle rate in normal cells, which would be oppositional to the effect seen *in vitro* in cancer cells (Scheppach *et al.* 1995), is not supported by this model. As such this revised model offers enlarged scope for application in identification of the biological basis of crypt compositional perturbation in early neoplasia, in response to the physiological microenvironment and leading to epithelial breakdown in inflammatory disease.

Author contributions

KS wrote successive iterations of the model, undertook model fitting to experimental data and wrote the paper; BMC generated relationships between cell types, evaluated iterations of the model and applications and wrote the paper. The authors declare no conflict of interest.

Acknowledgements

KS is grateful for the financial support of the EU FP7 (KBBE) Grant 289434 ‘BioPreDyn: New Bioinformatics Methods and Tools for Data-Driven Predictive Dynamic Modelling in Biotechnological Applications’. BMC undertook this work as a visiting researcher to MCISB.

References

- Anini Y., Fu-Cheng X.M., Cuber J.C., Kervran A., Chariot J. & Roze C. (1999) Comparison of the postprandial release of peptide YY and proglucagon-derived peptides in the rat. *Pflugers Arch.* **438**, 299–306.
- Bernstein C., Bernstein H., Payne C.M. & Garewal H. (2000) Field defects in progression to adenocarcinoma of the colon and esophagus. *Electron. J. Biotech.* **3**, 3.
- Buske P., Galle J., Barker N., Aust G., Clevers H. & Loeffler M. (2011) On the biomechanics of stem cell niche formation in the gut – modelling growing organoids. *PLoS Comput. Biol.* **7**, e1001045.
- Cho K.-H., Lee H.-S. & Ku S.-K. (2008) Decrease in intestinal endocrine cells in Balb/c mice with CT-26 carcinoma cells. *J. Vet. Sci.* **9**, 9–14.
- Corfe B.M., Williams E.A., Bury J.P. *et al.* (2009) A study protocol to investigate the relationship between dietary fibre intake and fermentation, colon cell turnover, global protein acetylation and early carcinogenesis: the FACT study. *BMC Cancer* **9**, 332.
- De Matteis G., Graudenzi A. & Antoniotti M. (2013) A review of spatial computational models for multi-cellular systems, with regard to intestinal crypts and colorectal cancer development. *J. Math. Biol.* **66**, 1409–1462.
- Dunn S.J., Appleton P.L., Nelson S.A., Nätke I.S., Gavaghan D.J. & Osborne J.M. (2012) A two-dimensional model of the colonic crypt accounting for the role of the basement membrane and pericryptal fibroblast sheath. *PLoS Comput. Biol.* **8**, e1002515.
- Fishwick P.A. (2012) Hypermodelling: an integrated approach to dynamic system modelling. *J. Simul.* **6**, 2–8.
- Gibson P.R., Moeller I., Kagelari O., Folino M. & Young G.P. (1992) Contrasting effects of butyrate on the expression of phenotypic markers of differentiation in neoplastic and nonneoplastic colonic epithelial-cells *in vitro*. *J. Gastroenterol. Hepatol.* **7**, 165–172.
- Gulubova M. & Vlaykova T. (2008) Chromogranin A-, serotonin-, synaptophysin- and vascular endothelial growth factor-positive endocrine cells and the prognosis of colorectal cancer: an immunohistochemical and ultrastructural study. *J. Gastroenterol. Hepatol.* **23**, 1574–1585.
- Gunawardene A.R., Corfe B.M. & Staton C.A. (2011) Classification and functions of enteroendocrine cells of the lower gastrointestinal tract. *Int. J. Exp. Pathol.* **92**, 219–231.
- Hague A., Singh B. & Paraskeva C. (1997) Butyrate acts as a survival factor for colonic epithelial cells: further fuel for the *in vivo* versus *in vitro* debate. *Gastroenterology* **112**, 1036–1040.
- Hamer H.M., Jonkers D., Venema K., Vanhoutvin S., Troost F.J. & Brummer R.J. (2008) Review article: the role of butyrate on colonic function. *Aliment. Pharmacol. Ther.* **27**, 104–119.
- Holt P.R., Atillasoy E., Lindenbaum J. *et al.* (1996) Effects of acarbose on fecal nutrients, colonic pH, and short-chain fatty acids and rectal proliferative indices. *Metabolism* **45**, 1179–1187.
- Hoops S., Sahle S., Gauges R. *et al.* (2006) COPASI – a COMplex PATHway Simulator. *Bioinformatics* **22**, 3067–3074.
- Hucka M., Finney A., Sauro H.M. *et al.* (2003) The systems biology markup language (SBML): a medium for representation and exchange of biochemical network models. *Bioinformatics* **19**, 524–531.
- Humphries A. & Wright N.A. (2008) Colonic crypt organization and tumorigenesis. *Nat. Rev. Cancer* **8**, 415–424.
- Inagaki A. & Sakata T. (2005) Dose-dependent stimulatory and inhibitory effects of luminal and serosal n-butyric acid on epithelial cell proliferation of pig distal colonic mucosa. *J. Nutr. Sci. Vitaminol.* **51**, 156–160.

- Johnston M.D., Edwards C.M., Bodmer W.F., Maini P.K. & Chapman S.J. (2007a) Mathematical modeling of cell population dynamics in the colonic crypt and in colorectal cancer. *Proc. Natl. Acad. Sci. U S A* **104**, 4008–4013.
- Johnston M.D., Edwards C.M., Bodmer W.F., Maini P.K. & Chapman S.J. (2007b) Examples of mathematical modeling – tales from the crypt. *Cell Cycle* **6**, 2106–2112.
- Li C., Donizelli M., Rodriguez N. *et al.* (2010) BioModels Database: an enhanced, curated and annotated resource for published quantitative kinetic models. *BMC Syst. Biol.* **4**, 92.
- Mirams G.R., Fletcher A.G., Maini P.K. & Byrne H.M. (2012) A theoretical investigation of the effect of proliferation and adhesion on monoclonal conversion in the colonic crypt. *J. Theor. Biol.* **312**, 143–156.
- Pin C., Watson A.J. & Carding S.R. (2012) Modelling the spatio-temporal cell dynamics reveals novel insights on cell differentiation and proliferation in the small intestinal crypt. *PLoS ONE* **7**, e37115.
- Sakata T. (1987) Stimulatory effect of short chain fatty-acids on the epithelial-cell proliferation in rat intestine – a possible explanation for trophic effects of fermentable fiber, gut microbes and luminal trophic factors. *Br. J. Nutr.* **58**, 95–103.
- Sakata T. & von Engelhardt W. (1983) Stimulatory effect of short chain fatty-acids on the epithelial-cell proliferation in rat large-intestine. *Comp. Biochem. Physiol. A Comp Physiol* **74**, 459–462.
- Sandler R.S., Baron J.A., Tosteson T.D., Mandel J.S. & Haile R.W. (2000) Rectal mucosal proliferation and risk of colorectal adenomas: results from a randomized controlled trial. *Cancer Epidemiol. Biomarkers Prev.* **9**, 653–656.
- Scheppach W., Bartram H.P. & Richter F. (1995) Role of short-chain fatty acids in the prevention of colorectal cancer. *Eur. J. Cancer* **31A**, 1077–1080.
- Smallbone K., Mendes P. (2013) Large-scale metabolic models: from reconstruction to differential equations. *Ind. Biotechnol.* **9**, 179–184.
- Tomlinson I.P.M. & Bodmer W.F. (1995) Failure of programmed cell-death and differentiation as causes of tumors – some simple mathematical models. *Proc. Natl. Acad. Sci. USA* **92**, 11130–11134.
- Yu D.C., Bury J.P., Tiernan J., Waby J.S., Staton C.A. & Corfe B.M. (2011) Short-chain fatty acid level and field cancerization show opposing associations with enteroendocrine cell number and neuropilin expression in patients with colorectal adenoma. *Mol. Cancer* **10**, 27.

Supporting information

Additional Supporting Information may be found in the online version of this article:

Figure S1. Observational data from our ongoing and previously published work were used to establish a set of assessment criteria (relevant compartments, capacity of crypts and direction and strength of relationships between compartments) by which any revision of the model could be objectively assessed.

Figure S2. Lack of fit of existing model to observed data.

Figure S3. Sensitivity Analysis of model v3.